Data-Driven Analysis of Chaotic Orbits in the Circular Restricted Three Body Problem

Urashi Taiki,* Bando Mai† and Hokamoto Shinji‡
Kyushu University, Fukuoka, Japan, 819-0395

November 29, 2021

Abstract

This paper analyzes ballistic lunar transfers known as chaotic orbits by using a data-driven approach called HAVOK (Hankel Alternative View of Koopman). HAVOK is a method to decompose a chaotic dynamical system into a linear model with intermittent forcing, and it has a possibility to reveal the chaotic dynamical system. In this analysis, chaotic orbits can be reconstructed by HAVOK, and the transport mechanism of them is clarified by classifying the magnitude of the intermittent forcing. In addition, the relation between the transport mechanism obtained by HAVOK and the dynamical structure of the circularly restricted three-body problem is revealed by periapsis Poincaré map.

1 Introduction

Recently, low-energy orbits called the ballistic lunar transfers have attracted much attention for its use in actual missions. The conventional method, Hohmann transfer, has the disadvantage of high cost due to the need for insertion burning. On the other hand, the ballistic lunar transfers are achieved only by the gravitational attractions of the Earth, the Moon, and other planets, so they don't require orbit insertion maneuver, and have low cost and high safety. In 1995, Bolt and Meiss found a chaotic Earth-Moon transfer orbit that achieves ballistic capture and that requires 38 % less total velocity boost than a comparable Hohmann transfer orbit.[1] However, the ballistic lunar transfers require a huge amount of time to reach the Moon. In order to solve this problem, research has been done on it, but the dynamics of ballistic lunar transfers have not yielded many valid results, because the low-energy transit from the Earth region to the Moon region is caused by a chaotic process called lunar gravitational capture (the phenomenon of temporarily staying near the Moon). In 2006, Ross designed a lower cost orbit by con-

sidering the invariant manifold of Lyapunov orbit around L_1.[2] In addition, in 2017, Oshima designed an orbit that considers the gravitational assist due to resonant orbits in addition to the invariant manifold of Lyapunov orbit.[3] This paper proposes a new approach to analysis by data, which is different from such dynamical analysis.

Chaotic systems, which are also treated in this paper, exist in every field of physics, biology, and engineering. For example, planetary motion, weather, financial markets, and epidemiology are known as chaotic phenomena. In the fields of climate science and neuroscience, data-driven analysis is actively pursued because the laws of physics and governing equations are still unclear, although there is a wealth of data. In classical fields such as turbulence, where governing equations exist, data-driven analysis is also being actively conducted.

DMD (Dynamic Mode Decomposition) is a method of mode decomposition of a nonlinear system from time series data without using the governing equations.[4] It was developed in the field of fluid dynamics in 2016 by Kutz et al, which can decompose high-dimensional, nonlinear time series data obtained from dynamic systems into multiple modes with frequencies and decay rates. However, although DMD is effective to obtain a global linear representation of a nonlinear system, it is not sufficient to describe a chaotic system with stronger nonlinearity. To solve this problem, HAVOK (Hankel alternative view of Koopman), a method to decompose chaotic systems into linear models with intermittent forcing, was proposed by Bruton et al. in 2017.[5] Then HAVOK has been applied to various chaotic systems such as EEG, double pendulum, and measles. By applying, a linear representation of the chaotic system was obtained, and as a result, the chaotic phenomenon was successfully predicted.[5] Thus, obtaining a global linear representation of a chaotic system is an innovative possibility.

This paper applies HAVOK to the chaotic orbits of the circularly restricted three-body problem of the Earth-Moon system, and brings new insights to the analysis and design of ballistic lunar transfers. First, the chaotic orbit is modeled as the linear regression model to indicate the usefulness of HAVOK. Next, the transition mechanism is clarified by analyzing the input of HAVOK. Moreover, a comparison with the analysis using the dynamical struc-

---

*Graduate student, Department of Aeronautics and Astronautics, Kyushu University, urashi.taiki.059@s.kyushu-u.ac.jp

†Associate Professor, Department of Aeronautics and Astronautics, mbando@aero.kyushu-u.ac.jp, Member AIAA.

‡Professor, Department of Aeronautics and Astronautics, hokamoto@aero.kyushu-u.ac.jp, Member AIAA.

ture is conducted to investigate what the input means in terms of dynamics.

2 theory

2.1 DMD

DMD is a data-driven method for mode decomposition of a nonlinear system from time series data without using governing equations. Therefore, it enables the analysis, prediction, and control of nonlinear dynamical systems.[4] DMD linearizes the time series data x_k by constructing the state transition matrix A as shown equation (1).

$$\boldsymbol{x_{k+1}} = A\boldsymbol{x_k} \tag{1}$$

DMD uses the time series data x_k of the nonlinear dynamical system and stores it in the matrix X, X' by shifting it by one step as follows.

$$X = \begin{bmatrix} | & | & & | \\ x_1 & x_2 & \ldots & x_{m-1} \\ | & | & & | \end{bmatrix} \tag{2}$$

$$X' = \begin{bmatrix} | & | & & | \\ x_2 & x_3 & \ldots & x_m \\ | & | & & | \end{bmatrix} \tag{3}$$

By equation (1),

$$X' = AX \tag{4}$$

Using the pseudo-inverse matrix $X^\dagger$,

$$A = X'X^\dagger \tag{5}$$

In this way, the state transition matrix A is computed by least-squares. By finding the eigenvalues and eigenvectors of A, the mode of the system can be determined.

2.2 HAVOK

HAVOK analysis provides a data-driven decomposition of chaotic dynamical system into a forced linear system.[5] In HAVOK analysis, time-delay embedding of the time-series data is used by applying singular value decomposition to a Hankel matrix as shown Fig.1. Eigen-time-delay coordinates are obtained from a time series data $x(t)$ by taking a singular value decomposition of the Hankel matrix:

$$\boldsymbol{H} = \begin{bmatrix} x(t_1) & x(t_2) & \cdots & x(t_p) \\ x(t_2) & x(t_3) & \cdots & x(t_{p+1}) \\ \vdots & \vdots & \ddots & \vdots \\ x(t_q) & x(t_{q+1}) & \cdots & x(t_{p+q-1}) \end{bmatrix} = U\Sigma V^* \tag{6}$$

Then a linear model is constructed on the first $r-1$ variables and let the last variable, v_r, to act as a forcing term:

$$\frac{d}{dt}\boldsymbol{v}(t) = A\boldsymbol{v}(t) + Bv_r(t) \tag{7}$$

where $\boldsymbol{v} = [v_1 \quad v_2 \quad \cdots v_{r-1}]^T$ is a vector of the first $r-1$ eigen-time-delay coordinates. The r-th coordinate v_r is used an input forcing to the linear dynamics, which serves as a driven force of a chaotic behavior. The matrices A and B in the linear regression model (7) can be obtained by the standard dynamic mode decomposition (DMD) algorithm[4] or other algorithms, such as Sparse Identification of Nonlinear Dynamics (SINDy).[6]
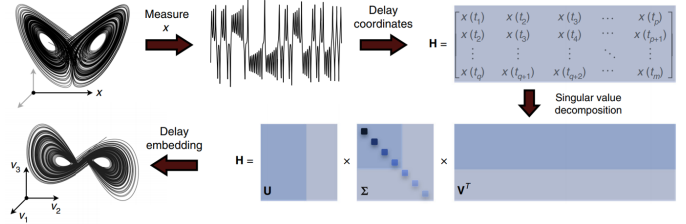
Figure 1: Procedure for obtaining the time delayed embedded attractor.[5]

2.3 Circular restricted three-body problem

The equations of motion of the circular restricted three-body problem (CRTBP) of are expressed by[7]

$$\begin{aligned} \ddot{x} - 2\dot{y} &= \frac{\partial U}{\partial x} \\ \ddot{y} - 2\dot{x} &= \frac{\partial U}{\partial y} \\ \ddot{z} &= \frac{\partial U}{\partial z} \end{aligned} \tag{8}$$

where U is the potential function defined by

$$\begin{aligned} U &= \frac{1}{2}\left(x^2 + y^2\right) + \frac{1-\mu}{r_1} + \frac{\mu}{r_2} \\ r_1 &= \sqrt{(x+\mu)^2 + y^2 + z^2} \\ r_2 &= \sqrt{(x-1+\mu)^2 + y^2 + z^2} \end{aligned}$$

x, y, and z are the position components of the spacecraft, r_1 and r_2 are the distances of the spacecraft with respect to the Earth and Moon. Given the masses of Earth and Moon by m_E and m_M respectively, the mass parameter μ is given by $\mu = \frac{m_M}{m_E+m_M}$. Integral of motion exists in the CR3BP, which is called Jacobi constant and is given by

$$C = 2U - (\dot{x}^2 + \dot{y}^2 + \dot{z}^2) \tag{9}$$

3 Results

3.1 Analysis of chaotic orbits by HAVOK

This section shows the result of applying HAVOK to the chaotic orbits in the circularly restricted three-body problem of the Earth-Moon system. First, solve the equation (8) with the initial condition (10) to obtain the orbit data

2

(Fig.2). From the equation (9), $C = 3.1726$. This orbit starts from the Earth regions, and then transits to the Moon regions by using the chaotic transition phenomenon. The orbital data with chaotic behavior is used for this analysis.

$$
\begin{bmatrix}
x(0) \\
y(0) \\
z(0) \\
\dot{x}(0) \\
\dot{y}(0) \\
\dot{z}(0)
\end{bmatrix}
=
\begin{bmatrix}
0.73 \\
0.27 \\
0 \\
0 \\
0 \\
0
\end{bmatrix}
\tag{10}
$$
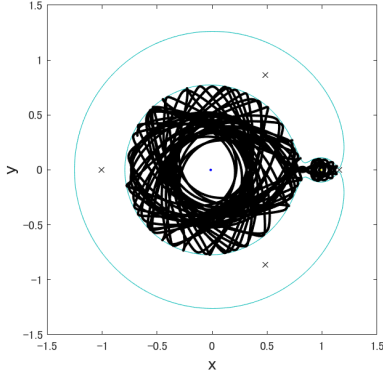
Figure 2: Chaotic orbit as data.

Next, the time delayed embedding attractor that is topologically equal to the original trajectory is obtained in order to build a linear regression model. First, one-dimensional time series data (distance from the Earth, $r = \sqrt{(x+\mu)^2 + y^2}$) is extracted from four-dimensional orbit data in Fig.3. Next, by stacking the time series data of r, the Hankel matrix shown in equation (6) is obtained. At this time, from the Takens embedding theory,[8] it is sufficient to have $(2 \times 4 + 1 =)$ 9 rows of time series data to stack. Then, the Hankel matrix is decomposed into singular values. The elements of V^T obtained by singular value decomposition are shown in (11). The singular value decomposition allows extracting the modes with the highest contribution to reconstructing the original orbit, and the delayed embedding attractor can be obtained by plotting the most dominant first and second lines in Fig.4. The attractor in which the positions of the Earth and the Moon are inverted is obtained.

$$
\boldsymbol{V^T} =
\begin{bmatrix}
v_1(t_1) & v_1(t_2) & v_1(t_3) & \cdots & v_1(t_p) \\
v_2(t_1) & v_2(t_2) & v_2(t_3) & \cdots & v_2(t_p) \\
\vdots & \vdots & \vdots & \ddots & \vdots \\
v_q(t_1) & v_q(t_2) & v_q(t_3) & \cdots & v_q(t_p)
\end{bmatrix}
\tag{11}
$$

Next, construct the linear regression model of the chaotic trajectory using V^T. The data of V^T is shifted by one step and stored in X and X', and the state transition matrix A is calculated by the least-squares method with $X' = AX$. Then, the forced input v_r is explained.

Figure 5 shows the time-series data for each row of V^T. It can be seen that the mode is intermittent after v_4. Hence, v_4 is considered as the forcing input. Finally, classify the state transition matrix A into the A, which makes accurate linear predictions, and the B, which corresponds to the forced input v_4, and construct the linear regression model with the forcing term as in the equation (12).

$$
\begin{bmatrix}
v_1 \\
v_2 \\
v_3
\end{bmatrix}_{k+1}
= A
\begin{bmatrix}
v_1 \\
v_2 \\
v_3
\end{bmatrix}_{k}
+ Bv_4
\tag{12}
$$

$$
A =
\begin{bmatrix}
1.0000 & 0.0005 & 0.0000 \\
-0.0005 & 1.0000 & 0.0037 \\
0.0000 & -0.0037 & 1.0000
\end{bmatrix}
, B =
\begin{bmatrix}
0.0000 \\
0.0000 \\
-0.0163
\end{bmatrix}
\tag{13}
$$
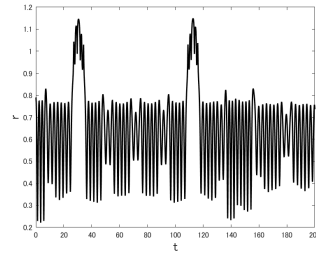
Figure 3: Time series data of r.
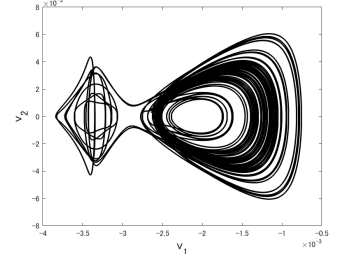
Figure 4: time delay embedding attractor.
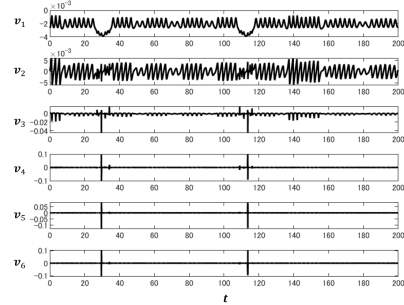
Figure 5: Time series data from v_1 to v_6.

3.2 Transition mechanism of the chaotic orbit

Here is the reconstruction of the time delayed embedding attractor by the linear regression model. First, in order to confirm that the chaotic transition phenomenon is caused by the forced input, the time delayed embedded attractor is reconstructed by the equation excluding the forced term in the second term of equation (12) in Fig.6(a). This attractor converges to the origin because the magnitude of the eigenvalues of the state transition matrix A is smaller than 1.

3

Next, the time delayed embedding attractor is reconstructed by equation (12) including the forcing term in Fig.6(b). Then, the Earth region and the Moon region can be distinguished, and the transition phenomenon can be confirmed. This indicates that the forcing input contributes to the chaotic transition phenomenon.

(a) Without forcing term. (b) With forcing Term.
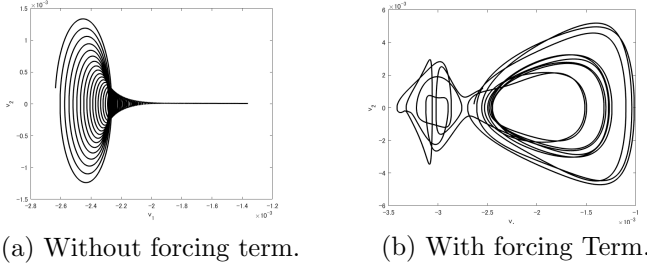
Figure 6: Reconstructing the time delayed embedded attractor with linear regression models.

In order to investigate how the forced input v_4 affects the trajectories, the input is divided into four categories according to its amplitude and period. Figure 7 shows the color classification of the forcing input. The black represents the large input, the blue represents the subtle input, the red represents the small input, and the pink represents the input at the Moon. Next, the time delayed embedded attractor (Fig.6(b)) reconstructed by the linear regression model(12) is colored at the same time in Fig.8. The bold line indicates the location where the input is active. First, it starts from the black trajectory and moves outward with the large input. Next, it moves to the inner blue trajectory, where it receives the subtle input. Then it moves to the middle red trajectory with the small input. Finally, it transitions from the red trajectory to the moon. In conclusion, the transition mechanism on the time delayed embedding attractor is that it goes from the outside to the inside, passes through the middle trajectory, and then transitions to the Moon. Finally, the actual orbits are also colored in the same way and shown in the Fig 9. The forcing input is due to the gravitational effects of the two objects, since no velocity change is added to the analysis. The large black input occurs near the Earth, and the small blue input occurs far away from the Earth. The orbit that receives the small red input is in the middle of the two orbits. In the actual orbit, the transition mechanism was found to be from a near-Earth orbit to a far-Earth orbit, then to the middle orbit, and then to the Moon. Furthermore, Figure 10 propagated the orbit longer and colored it in the same way. It shows that the relationship between the color and the distance from the Earth is the same. In this orbit, the black orbit near the Earth and the blue orbit far from the Earth do not transit to the Moon region.
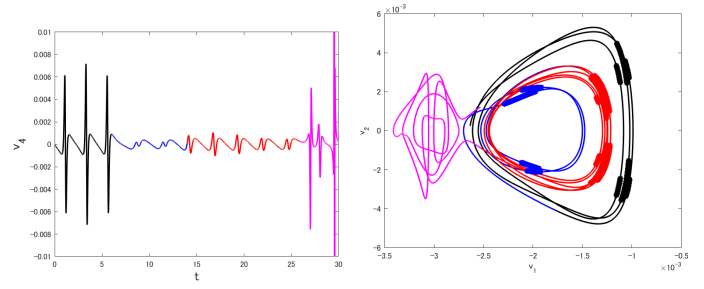
Figure 7: Color classification of v_4.

Figure 8: Color classification of the time delayed embedding attractor by input.
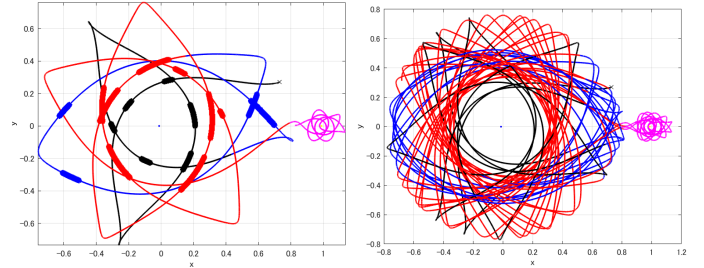
Figure 9: Color coding of the orbit.

Figure 10: Color coding of the longer orbit.

4   consideration

In this section, in order to investigate the dynamical implications of the forced input, a comparison with previous studies on dynamical analysis is conducted. Therefore, tube dynamics and lobe dynamics, which are the dynamical structures in the circularly restricted three-body problem, are introduced.

4.1   Tube Dynamics and Lobe Dynamics

Focusing on the unstable L_1 among the equilibrium points, and obtain a periodic orbit called the Lyapunov orbit around L_1 with the same Jacobi constant. Then, extract the structure of the phase space called the invariant manifold extending from the Lyapunov orbit. Periodic orbits and invariant manifolds are important structures such as "tube" that determine the flow of orbits in the phase space of dynamical systems with embedded chaotic orbits. In other words, an orbit with state quantity inside the tube transits through the tube to the Moon without the thrust.

In order to use the tube structure, it is necessary to raise the altitude of the spacecraft to the region where the tube exists. Resonant gravity assist is one of the methods to achieve this. By using a resonant state in which the period of the object and the spacecraft is expressed by a simple integer ratio, multiple gravity assists can be performed in a short time, and the semi-major axis of the spacecraft around the Earth can be increased up to the existence of the tube. Figure 12 and 13 show the resonant orbit with the ratio of the period of the moon and

4

spacecraft of 1:3 and 2:5. Then, the region surrounded by the stable and unstable manifolds of the resonant orbit is called Lobe, and the orbit with the state quantity inside Lobe can change the semi-major axis a efficiently due to the lunar gravity assist.
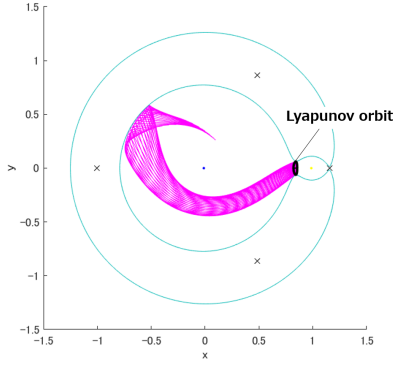
Figure 11: Stable manifolds (tube) extending from Lyapunov orbits.
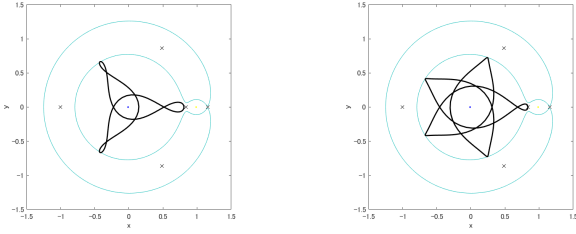
Figure 12: 1:3 resonant orbit. Figure 13: 2:5 resonant orbit.

4.2   Periapsis poincaré map

To distinguish whether the state quantity of an orbit are inside the tube and Lobe, the periapsis map is used. The periapsis map is an analysis method that extracts information at the periapsis ($\dot{r} = 0$) of the orbit. Radial velocity $\dot{r}$ is expressed by

$$\dot{r} = \frac{d}{dt}(\sqrt{(x+\mu)^2 + y^2 + z^2}) \qquad (14)$$
$$= \frac{(x+\mu)\dot{x} + y\dot{y} + z\dot{z}}{\sqrt{(x+\mu)^2 + y^2 + z^2}}$$

In the periapsis map, the vertical axis is the semi-major axis a in the Earth region, and the horizontal axis is the angle θ between the x-axis and the spacecraft centred on the Earth. θ is expressed by

$$\theta = \tan^{-1}(\frac{y}{x+\mu}) \qquad (15)$$

Therefore, the radial velocity v_r and the tangential velocity v_θ in the inertial coordinate system are

$$v_r = \dot{x}\cos\theta + \dot{y}\sin\theta \qquad (16)$$
$$v_\theta = r_1 - \dot{x}\sin\theta + \dot{y}\cos\theta \qquad (17)$$

Hence, semi-major axis a is expressed by

$$a = \frac{r_1(1-\mu)}{2(1-\mu) - r_1(v_r^2 + v_\theta^2)} \qquad (18)$$

Figure 14 shows the periapsis map. The orange points indicate the periapsis obtained by propagating multiple orbits with the same Jacobi constant as the analyzed orbit. The initial values for multiple orbits are

$$
\begin{bmatrix}
x(0) \\
y(0) \\
z(0) \\
\dot{x}(0) \\
\dot{y}(0) \\
\dot{z}(0)
\end{bmatrix}
=
\begin{bmatrix}
x \\
1.0 \times 10^{-6} \\
0 \\
0 \\
\sqrt{(x(0)^2 + (y(0)^2) + \frac{2(1-\mu)}{r_1} + \frac{2\mu}{r_2} - C} \\
0
\end{bmatrix}
\qquad (19)
$$

Figure 14 indicates that the regions can be classified into torus and discrete. Then the orbits obtained from the former region are periodic orbits, and the orbits obtained from the latter region are chaotic orbits. Moreover, Figure 14 shows the periapsis of the various orbits. The pink points indicate the periapsis of the tube. The ten triangle points indicate the periapsis of the analyzed orbit until the transition to the Moon, and are color-coded according to the magnitude of the forcing input for HAVOK. The green points indicate the periapsis of the resonant orbit for each resonance ratio. From fig.14,it can be confirmed that the 10th periapsis is inside the tube, indicating that the analyzing orbit uses the tube structure to transition to the Moon.

Next, in Fig.15 and Fig.16, the 1:3 and 2:5 lobes are drawn on the periapsis map. The green and red points respectively show the periapsis of the stable and unstable manifolds of the resonant orbit. In other words, the region surrounded by red and green points is the lobe. From these figures, it can be seen from Fig.15 that this orbit is not obviously inside the 1:3 lobe, but from Fig.16, the 2:5 lobe is used to convert the semi-major axis a. In detail, it can be seen that the color classification based on the magnitude of the forcing input corresponds to the transport structure of the semi-major axis a due to the lobe dynamics. In other words, it is clear that the forced input obtained by HAVOK models the "resonant hopping" phenomenon[9] due to lobe dynamics in terms of dynamics.

5
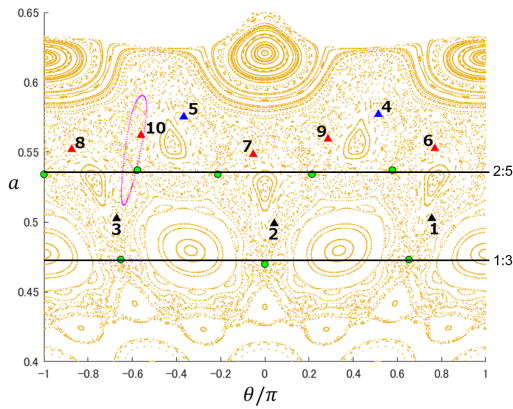
Figure 14: The periapsis Poincaré map of the multiple orbits ($C = 3.1726$).
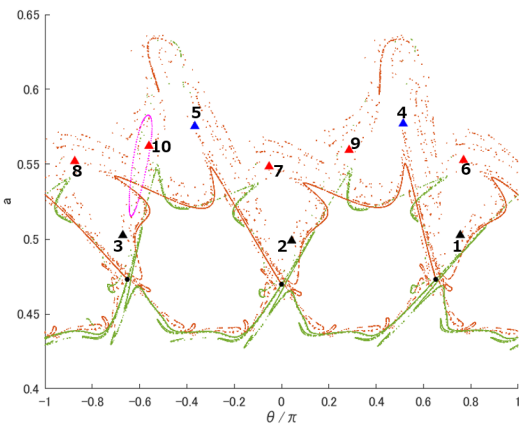
Figure 15: 1:3 lobes.

Figure 16: 2:5 lobes.

5   Conclusion

This paper applied HAVOK, a data-driven approach, to chaotic orbits in the Earth-Moon system and provided new insights into the low-cost trajectory design for ballistic lunar transfers. HAVOK enabled the chaotic trajectory to be decomposed into a linear model with a forcing term, therefore the usefulness of HAVOK in chaotic dynamical systems is demonstrated. Moreover, since the forcing input contributes to the chaotic transition phenomenon, by classifying the magnitude of the forcing input, it was found that the chaotic orbit has the transition mechanism. Furthermore, comparison with the dynamical analysis using the periapsis poincaré map showed that the forced input models the transport structure with changing semi-major axis a due to lobe dynamics.

The data-driven approach has the possibility to identify the underlying structure of complex dynamical systems and it helps to design transfer trajectories in the multi-body regime. It also has the possibility to address other challenges in the astrodynamics field, such as complex trajectory design, control and optimization.
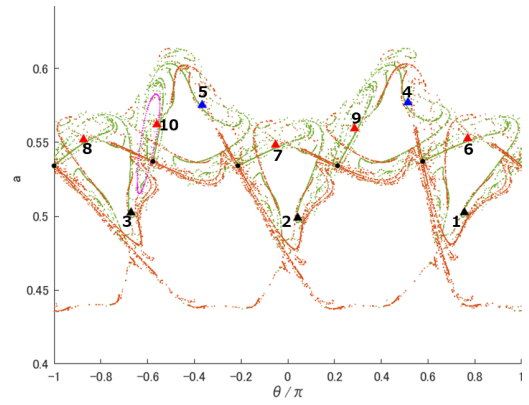
References

[1] E. M. Bollt and J. D. Meiss, "Targeting chaotic orbits to the Moon through recurrence," *Physics Letters A*, Vol. 204, No. 5-6, 1995, pp. 373–378.

[2] S. D. Ross and D. J. Scheeres, "Multiple gravity assists, capture, and escape in the restricted three-body problem," *SIAM Journal on Applied Dynamical Systems*, Vol. 6, No. 3, 2007, pp. 576–596.

[3] K. Oshima, S. Campagnola, and T. Yanao, "Global search for low-thrust transfers to the Moon in the planar circular restricted three-body problem," *Celestial Mechanics and Dynamical Astronomy*, Vol. 128, No. 2, 2017, pp. 303–322.

[4] J. N. Kutz, S. L. Brunton, B. W. Brunton, and J. L. Proctor, *Dynamic mode decomposition: data-driven modeling of complex systems*. SIAM, 2016.

[5] S. L. Brunton, B. W. Brunton, J. L. Proctor, E. Kaiser, and J. N. Kutz, "Chaos as an intermittently forced linear system," *Nature communications*, Vol. 8, No. 1, 2017, pp. 1–9.

[6] S. L. Brunton, J. L. Proctor, and J. N. Kutz, "Discovering governing equations from data by sparse identification of nonlinear dynamical systems," *Proceedings of the national academy of sciences*, Vol. 113, No. 15, 2016, pp. 3932–3937.

[7] J. Prussing and B. Conway, *Orbital Mechanics*, ch. 4, pp. 65–66. New York: Oxford University Press, 2 ed., 2013.

[8] L. Noakes, "The Takens embedding theorem," *International Journal of Bifurcation and Chaos*, Vol. 1, No. 04, 1991, pp. 867–872.

[9] R. L. Anderson, "Approaching moons from resonance via invariant manifolds," *Journal of Guidance, Control, and Dynamics*, Vol. 38, No. 6, 2015, pp. 1097–1109.